

# Continuous and Selective Removal of Lead from Drinking Water by Shock Electrodialysis

Huanhuan Tian, Mohammad A. Alkhadra, Kameron M. Conforti, and Martin Z. Bazant\*

Cite This: *ACS EST Water* 2021, 1, 2269–2274

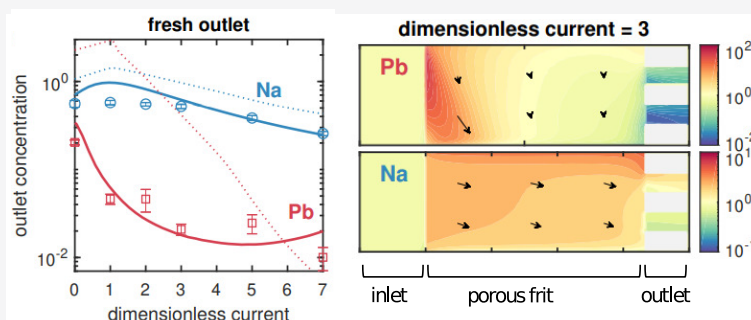
Read Online

ACCESS |

Metrics &amp; More

Article Recommendations

Supporting Information



**ABSTRACT:** The affordable and effective removal of traces of toxic heavy metal ions, especially lead, from contaminated drinking water in the presence of excess sodium or other competing ions has been a long-standing goal in environmental science and engineering. Here, we demonstrate the possibility of continuous, selective, and economical removal of lead from dilute feedwater using shock electrodialysis. For models of lead-contaminated tap water, this process can remove approximately 95% of dissolved lead (to safe levels below 1 ppb), compared to 40% of sodium ions, at 60% water recovery and at an electrical energy cost of only 0.01 kWh m<sup>-3</sup>. We are able to fit and interpret the separation data with a pore-depth-averaged electrokinetic model that reveals the mechanisms for selective separation of lead ions. This selectivity is enabled by the faster transport of lead ions from the charged porous medium to the cathode stream, as well as their larger barrier to escape to the fresh stream compared to sodium ions. The experimental and theoretical results could be used to guide the development of low-cost, point-of-use systems for continuous removal of lead from municipal water.

**KEYWORDS:** shock electrodialysis, lead contamination, electrokinetics

## INTRODUCTION

Excessive exposure to heavy metals such as lead affects the normal function of the human body and leads to heavy metal poisoning.<sup>1,2</sup> The most common means of unhealthy exposure to lead is by consumption of lead ions (Pb<sup>2+</sup>) present in contaminated drinking water.<sup>3–5</sup> Lead contamination of municipal water commonly results from the corrosion of plumbing elements, such as pipes, fixtures, faucets, and parts joined by lead solder.<sup>4</sup> For example, households in Flint, MI, and public schools across the United States, many of which still rely on legacy lead pipes for plumbing and transporting water, were recently exposed to dangerously high levels of lead in their drinking water.<sup>5,6</sup> This public health crisis has been addressed temporarily by distributing bottled water and expensive filters to residents and schools,<sup>7</sup> but more sustainable and cost-effective solutions are still in critical need. Conventional methods for the removal of lead from tap water, typically present in trace quantities, include filtration<sup>8–10</sup> and ion exchange,<sup>11–15</sup> though these systems are costly and require

either regular chemical regeneration or frequent replacement.<sup>16,17</sup>

In this work, we adapt an emerging method for electrokinetic deionization known as shock electrodialysis (shock ED)<sup>17–20</sup> to continuously and selectively remove lead from water in the presence of excess sodium, a common mineral necessary for normal body function. The main part of the system is a negatively charged macroporous material (the nominal pore size of which is  $\sim 1 \mu\text{m}$ ) sandwiched between two cation exchange membranes (CEMs), as shown in Figure 1. The negative surface charge attracts cations and repels anions, which produces the so-called electrical double layer

Received: July 10, 2021

Published: September 22, 2021



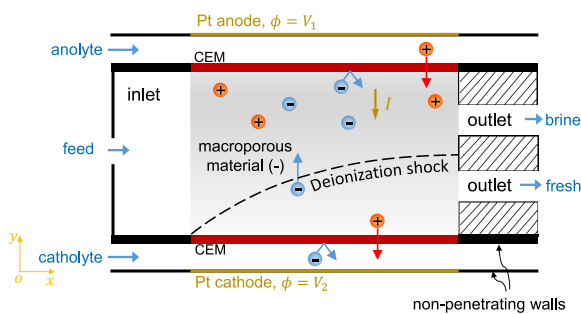


**Figure 1.** Schematic of the shock ED system.

(EDL). The EDL gives rise to various electrokinetic phenomena, such as surface conduction, electroosmosis (flow induced by an electrical field), diffusio-osmosis (flow induced by a concentration gradient), and streaming potential (an electrical field induced by the flow of an electrolyte). As an electrical current is applied to the system (e.g., via water splitting at the electrodes), ion concentration polarization occurs inside the porous material, and when the applied current exceeds the diffusion-limited current (which is made possible by surface conductance and electroosmosis<sup>21</sup>), a deionization shock wave propagates from the cathode-side membrane to the anode-side membrane.<sup>22,23</sup> A cross-feed stream of fluid can then be split into fresh and brine products at the outlet. As a comparison, traditional electrodialysis uses

alternating cation and anion exchange membranes that separate unsupported (without charged porous media) brine and fresh streams and requires greater energy for deionization due to the diffusion-limited current.

In 2015, Schlumpberger et al.<sup>18</sup> reported the first continuous shock ED prototype and achieved >99% deionization for binary electrolytes like NaCl and KCl. The scalings of total deionization and water recovery versus current have since been described by boundary-layer analysis and two-dimensional numerical simulation based on a simple homogenized model, where the EDL is assumed to be much thinner than the characteristic pore size,<sup>24</sup> but this approach is unable to predict the remarkable ion selectivity of shock ED. Recent experiments on mixtures of NaCl and MgCl<sub>2</sub>,<sup>17</sup> artificial seawater,<sup>20</sup> and nuclear process water<sup>19</sup> have shown that shock ED is highly selective in separating multivalent ions such as Mg<sup>2+</sup> and Co<sup>2+</sup> from mixtures with monovalent salts. As a result, the target ions can be effectively removed while maintaining a low level of electrical energy consumption because the other supporting ions maintain the conductivity of the solution. This fortuitous property makes shock ED competitive in applications that require selective removal of dilute multivalent contaminants.

Here, we exploit this unique feature of shock ED to achieve continuous, selective, low-cost removal of trace amounts of lead from dilute solutions of model tap water. The working conditions differ from previous works in terms of the very low concentration of the target species (Pb<sup>2+</sup>) compared to the excess competing ion (Na<sup>+</sup>; in molar units, Na<sup>+</sup>:Pb<sup>2+</sup> = 1350:1), as well as the overall low ionic strength of the feed

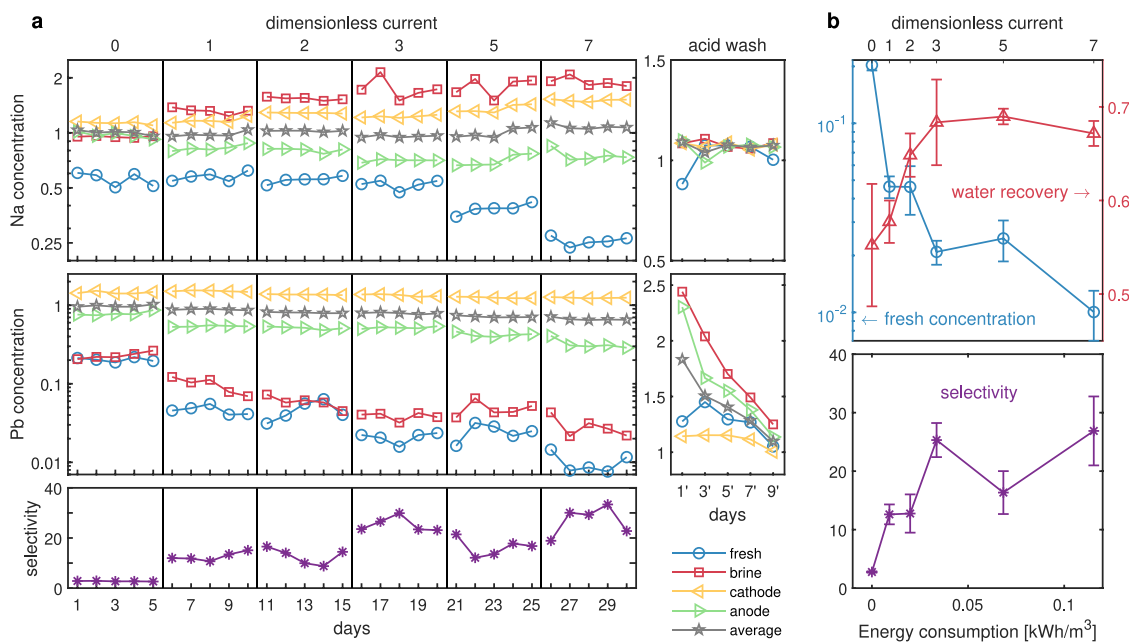


**Figure 2.** Experimental results for the removal of lead from water by the frit device. In panel a, the first two rows show the dimensionless outlet concentrations of Na<sup>+</sup> and Pb<sup>2+</sup> for the fresh, brine, cathode, and anode streams as well as the flow-weighted average concentration of the four streams, for a continuous 30-day run of the frit device at different dimensionless currents followed by a continuous 9-day acid wash of the frit device at zero current (all three inlet streams contain HCl at a concentration of 50 mM in addition to the mixture of Na<sup>+</sup> and Pb<sup>2+</sup>). These concentrations are all normalized by the inlet concentration of the corresponding ion, and the applied current is scaled by the flow-limiting current (20  $\mu$ A). The last row shows the ion removal selectivity for the 30-day run, which is defined by the ratio of dimensionless fresh outlet concentration of Na<sup>+</sup> to Pb<sup>2+</sup>. (b) Five-day averaged values and standard deviations of dimensionless lead fresh concentration, water recovery, and selectivity for each dimensionless current. The corresponding energy consumption is shown on the bottom axis.

( $\approx 0.18$  mM). For such dilute solutions, surface conduction is comparable with bulk conduction in the negatively charged macroporous medium, which enhances the selectivity. Our experimental data are quantitatively consistent with the predictions of a pore-cross-section-averaged model,<sup>25,26</sup> which reveals the underlying electrokinetic mechanisms for selectivity, based on different energy barriers and transport rates experienced by multivalent and monovalent ions passing through the system.

## MATERIALS AND EXPERIMENTAL METHODS

The device used here was fabricated following a design recently published by our group.<sup>17,19,20</sup> As shown schematically in Figure 1, this architecture comprised three inlets and four outlets. Two of the inlets and two of the outlets transported fluid across the electrodes, and the third inlet delivered contaminated feed to be purified. The two remaining outlets discharged the processed feed that was split into fresh and brine streams using an acrylic splitter. The electrodes were made of platinum mesh and connected to a Gamry Reference 3000 potentiostat/galvanostat using titanium wires, and the CEMs were Nafion N115. The ionic composition of the outlet was determined using inductively coupled plasma mass spectrometry (Agilent 7900 ICP-MS). For more details about the materials, assembly, fabrication, and measurement, see the Materials and Experimental Methods in ref 19. In this study, we used two different materials for the porous microstructure, namely, a borosilicate frit and a silicon carbide ceramic. The borosilicate frit was manufactured by Adams & Chittenden Scientific Glass and had ultrafine pores (nominally ranging from 0.9 to 1.4  $\mu\text{m}$  in size), an internal surface area of 1.75  $\text{m}^2 \text{g}^{-1}$  based on Brunauer–Emmett–Teller theory, a mass density of 1.02  $\text{g cm}^{-3}$ , a porosity of 48%, and dimensions of 0.5 cm ( $x$ )  $\times$  2 cm ( $y$ )  $\times$  1 cm ( $z$ ). The silicon carbide (SiC) ceramic was manufactured by Saint-Gobain Research and had a larger porosity of 56%, a bimodal pore size distribution (1–100 nm and 1–10  $\mu\text{m}$ ), and also dimensions of 0.5 cm ( $x$ )  $\times$  2 cm ( $y$ )  $\times$  1 cm ( $z$ ).

To model the conditions at the 90th percentile of tap water contaminated with lead in Flint, MI, during the water crisis,<sup>27,28</sup> the feed used in this paper was a mixture of lead and sodium with concentrations of approximately 28  $\mu\text{g L}^{-1}$  (28 ppb) and 4.2  $\text{mg L}^{-1}$  (4.2 ppm), respectively. Real tap water normally includes other ions and minerals, but this formulation is relevant to examine the continuous and selective lead removal in the presence of sodium as a competing ion. To create this mixture, we prepared stock solutions with 1000 times the target concentrations made from lead chloride ( $\text{PbCl}_2$ ) and sodium chloride ( $\text{NaCl}$ ), and appropriate volumes of these solutions were then diluted in deionized water. All reagents were purchased from MilliporeSigma and used as received. In the preparation of this mixture, the anolyte, catholyte, and contaminated feed were made identical in composition, though the catholyte alone was dosed with hydrochloric acid (HCl) at a concentration of 50 mM. This dose of HCl was added to prevent precipitation of lead oxides or hydroxides that could have formed due to hydrogen evolution in the otherwise basic catholyte. For the device comprising the borosilicate glass (SiC ceramic), the flow rate of the anolyte and catholyte was 180  $\mu\text{L min}^{-1}$  (230  $\mu\text{L min}^{-1}$ ), and that of the feed was 66  $\mu\text{L min}^{-1}$  (56  $\mu\text{L min}^{-1}$ ). We chose the flow limiting current  $I_{\text{lim}} = \sum_{\text{cations}} z_i F c_i Q \approx 20 \mu\text{A}$  as the characteristic current for a flow rate of 66  $\mu\text{L min}^{-1}$ .

**Experimental Results.** Figure 2a shows the outlet concentrations of  $\text{Na}^+$  and  $\text{Pb}^{2+}$  for all streams as well as the average concentration of the four streams, and the ion removal selectivity (which is defined by the ratio of the dimensionless fresh concentration of Na to Pb), for two operating conditions on the frit device. The left of this panel corresponds to a 30-day continuous run of the frit device at different dimensionless currents. Even at zero current, approximately 80% of the lead was removed, which was mainly due to the exchange of  $\text{Pb}^{2+}$  and  $\text{H}_3\text{O}^+$  across the membrane on the cathode side. The ion removal selectivity was 2–3. The mean outlet concentration was almost the same as the inlet concentration, which indicates that lead ions did not accumulate inside the frit. As the current was increased, more lead ions were removed from both the fresh and brine streams, where the concentration of  $\text{Pb}^{2+}$  was reduced to <1 ppb (>95% removal for both fresh and brine stream), and the selectivity reached  $\sim 30$ . This time, however, the mean outlet concentration of  $\text{Pb}^{2+}$  decreased, which suggests that  $\text{Pb}^{2+}$  accumulated inside the device. As a comparison,  $\text{Na}^+$  was removed less than  $\text{Pb}^{2+}$  (at most  $\sim 75\%$   $\text{Na}^+$  removal from the fresh stream), yet the former did not accumulate in the device. Possibly due to lead participation or other mechanisms, the pressure increased at the inlet of the frit with the current, and finally as we increased the dimensionless current to a value of 10, the device became clogged. To unclog the system, we introduced HCl into the feed and anode streams at a concentration of 50 mM (already present in the cathode stream) and decreased the feed flow rate to two-thirds of the original rate for several days. After we increased the flow rate to its original value, we recorded the outlet concentration for 10 days. As we can see from the right panel of Figure 2a, lead ions were released from the device, especially from the anode and brine streams, and no further clogging of the device was observed.

In addition to the extent of ion removal, we are interested in energy consumption and water recovery (defined as the fraction of water recovered from the feed as fresh product). Figure 2b shows the averaged fresh concentration of lead, water recovery, and ion removal selectivity, versus energy consumption per unit volume of feed for each dimensionless current during the 30-day run using the frit device. The water recovery increases with current (or energy consumption), which is explained by electroosmosis from the anode side to the cathode side in the negatively charged macroporous material (the overall positively charged fluid tends to move with the electric field). More than 95% of the lead was removed with >60% water recovery and >10 selectivity for an energy consumption of 0.01  $\text{kWh m}^{-3}$  and a dimensionless current of 1–2. Note that if 95% Na were also removed, this energy consumption would be much larger due to the increased resistance of the electrolyte. Under this low current, the accumulation of lead in the device is so slow (barely detectable over several days) that this is effectively a continuous process, in which the device would simply need to be refreshed by an acid wash after some period of operation, depending on the level of lead contamination. Alternatively, the gradual capture of lead in the relatively inexpensive and interchangeable porous material could also be leveraged periodically for safe disposal. We note, however, that we used acid while running the devices, which is an operating cost that can be eliminated by introducing and recycling a buffer solution, as we have demonstrated in previous work.<sup>20</sup> In that

case, there is no hydronium exchange at zero current and thus an applied current is necessary for ion removal.

Figure 3 shows the experimental results for a 30-day continuous run of the SiC device at zero electric current. The

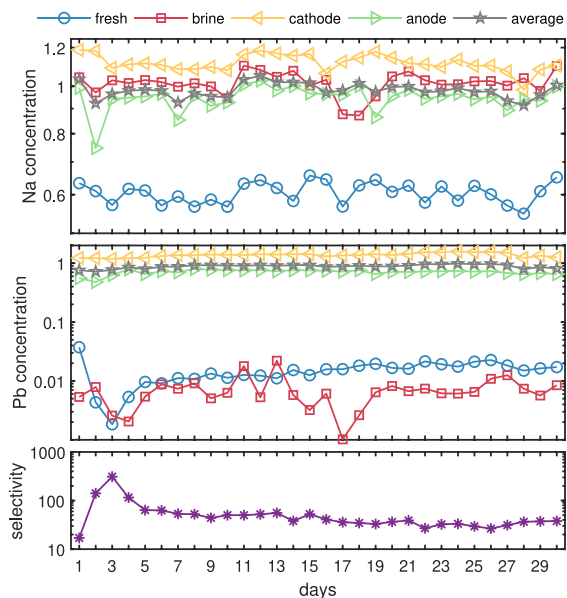


**Figure 3.** Experimental results for the removal of lead from water by the SiC device. No electric current was applied. The explanation of this figure can be found in Figure 2a.

SiC device removed >95% of  $\text{Pb}^{2+}$  (fresh concentration of <2 ppb) but only 40% of  $\text{Na}^+$ , indicating a selectivity of >30. Meanwhile, the dimensionless mean outlet concentration of lead was  $\sim 1$ , which indicates that lead did not accumulate in the device. Because 2 ppb is already well below the EPA action limit of 15 ppb, it was not necessary to apply current to the SiC device to further improve lead removal. The water recovery was approximately 80% possibly because the splitter was placed closer to the anode. The more selective lead removal by the SiC device compared with that of the frit device at zero current shows the potential to significantly improve shock ED performance by optimizing the materials, though the reasons are still to be investigated. Possible reasons include the advantages of bimodal pore distribution and different surface charges.

**Principles of Selective Lead Removal.** The experimental data of the frit device can be quantitatively interpreted using a pore-depth-averaged electrokinetic model,<sup>25,26</sup> which reveals the fundamental mechanisms for multivalent ion separation by shock ED using homogeneous porous material. The model uses the depth-averaged Poisson–Nernst–Planck–Stokes equations to describe three-dimensional transport in a microfluidic shock ED system. The model applies to multicomponent electrolytes for any EDL thickness, captures the phenomena of electroosmosis, diffusioosmosis, streaming potential, and water dissociation, and incorporates the inlet and outlet frit–electrolyte interface. We showed that this model can predict the experimental deionization and conductance for binary electrolytes well,<sup>18</sup> and we qualitatively demonstrated the selective removal of  $\text{Mg}^{2+}$  relative to  $\text{Na}^+$ .<sup>17</sup> The model parameters we used for this work are summarized

in the Supporting Information. Note that the model includes several important parameters that can be adjusted to fit the experimental data: the membrane hindrance factor (i.e., the ratio of effective diffusivity in the membrane to bulk diffusivity), the surface charge density ( $\sigma$ ) of the frit, and the membrane charge density. In the model, we assume a constant  $\sigma$  for the sake of simplicity, while in fact,  $\sigma$  can vary with the current and local ionic composition due to charge regulation.<sup>29</sup> In addition to the full depth-averaged model, we also calculated the homogenized model in which the EDL is assumed to be much thinner than the nominal pore size, and thus the depth-averaged coefficients are reduced to 1 or 0.<sup>25</sup> Homogenized models are regularly used in the literature due to their simplicity,<sup>22–24</sup> but they can miss important mechanisms for selective ion removal.<sup>26</sup> In this work (ionic strength of the feed stream of approximately 0.18 mM), the EDL thickness is on the order of 10–100 nm (comparable with  $h_p \approx 250$  nm, the inverse of pore area density), which means that the EDL occupies a significant part of the total pore volume. In this case, the pore-averaged concentrations can be very different from the bulk concentrations, which may be important for selective lead removal.

The simulation results of the full depth-averaged and homogenized models are shown in panels a and b of Figure 4. The depth-averaged model predicts selective lead removal for any current, and it quantitatively agrees with experimental data except for the concentration of lead in the brine stream for dimensionless currents of >3, possibly because the model does not capture the accumulation of lead in the device. The depth-averaged model also works well for the water recovery and current–voltage relationship. The homogenized model, on the contrary, shows no selective lead removal at low current, which indicates that the finite EDL thickness is a key feature of selective lead removal at low current. To analyze the mechanisms of selective lead removal, Figure 4c shows the contour maps of depth-averaged concentrations and relative fluxes at representative locations. As the cross-flow proceeds, the concentration of  $\text{Pb}^{2+}$  decreases more relative to that of  $\text{Na}^+$  in the charged channel, especially when the applied current is large. In addition, we observe a greater decrease in the concentration of  $\text{Pb}^{2+}$  compared to that of  $\text{Na}^+$  at the interface between the charged channel and the outlet, which suggests that  $\text{Pb}^{2+}$  is more preferably transported to the cathode stream than to the outlet. These two phenomena, in which lead ions are removed to a greater extent from the charged channel to the cathode stream (by ion exchange or electrical current) and they are harder to transport from the charged channel to the outlet, collectively explain the selective lead removal in the fresh stream by shock ED. The first phenomenon indicates that the surface charge is preferably balanced by monovalent cations in the shock ED system. Under the condition of weak charge and no electroosmosis, this can be quantitatively proven by a scaling analysis.<sup>26</sup> In the full problem in this work, the transport is more complicated, and the deionization shock is not even obvious because the inlet solution is so dilute that the weak charge condition ( $\frac{\sigma}{h_p F} \ll I_s^{\text{in}}$ , where  $F$  is Faraday constant and  $I_s^{\text{in}}$  is the inlet ionic strength)<sup>22</sup> is not satisfied. Therefore, we can just numerically show that the multivalent cations are more reduced in the charged channel (Figure 4c). On the contrary, the second phenomenon can be explained by two mechanisms<sup>26</sup> (Figure 4d). First, the multivalent lead ions are more strongly attracted

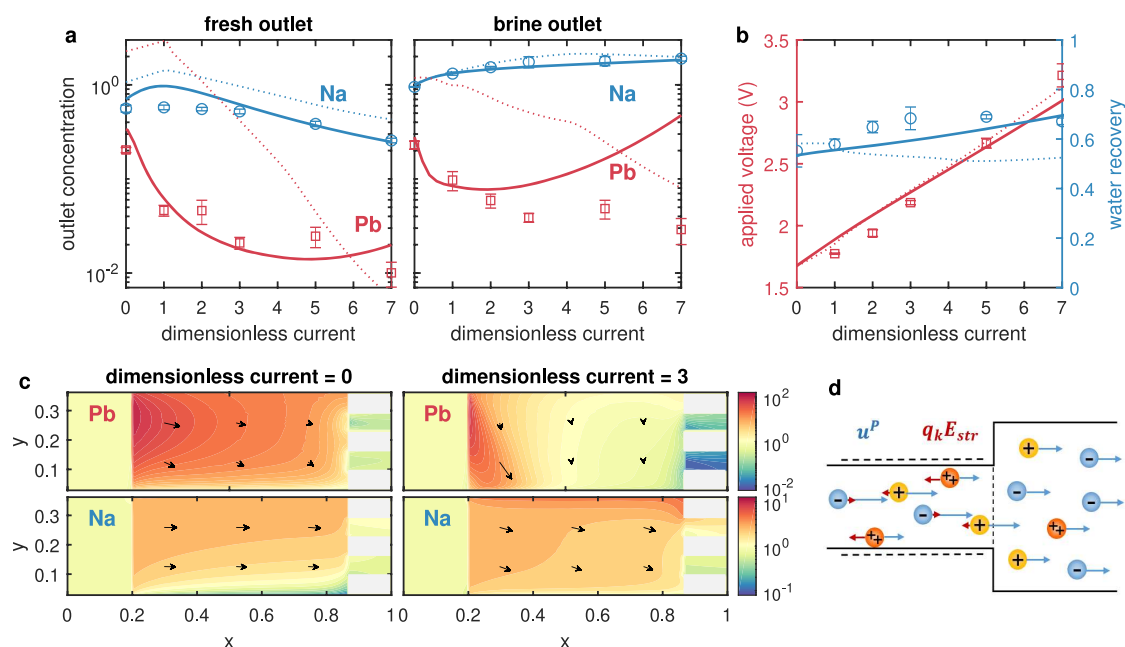


**Figure 4.** Simulation results of lead removal using the frit-based device. In panels a and b, the solid lines, dotted lines, and markers represent the full depth-averaged model, the homogenized model, and the five-day averaged experimental data, respectively. (a) Outlet concentrations (scaled by the corresponding inlet concentrations) of the fresh and brine streams vs dimensionless current. (b) Water recovery and applied voltage vs dimensionless current. The water dissociation potential of 1.5 V is added to the simulated values for voltage to compare with experiments. (c) Contour maps of dimensionless depth-averaged concentration and flux vectors at six sample locations in the frit for  $\text{Na}^+$  and  $\text{Pb}^{2+}$  at two different dimensionless currents; results were obtained using the full depth-averaged model. The frit is located between  $x = 0.2$  and  $0.867$ ; the light-gray blocks represent the splitter, and the electrode streams and membranes are not shown here. (d) Schematic showing ion transport by convection and streaming potential at the interface between a charged channel and the outlet.  $u^p$  is the pressure-driven flow velocity, and  $q_k E_{\text{str}}$  is the electrostatic force generated by streaming potential ( $q_k$  is the charge of ion species  $k$ , and  $E_{\text{str}}$  is the electrical field).

to the negatively charged pore surface, where the flow velocity is reduced due to the no-slip boundary. The depth-averaged coefficient  $\beta_k^p = \frac{\langle u^p c_k \rangle}{\langle u^p \rangle \langle c_k \rangle}$  provides a quantitative description of the difference between the depth-averaged convective flux  $\langle u^p c_k \rangle$  and the product of the depth-averaged velocity  $\langle u^p \rangle$  and concentration  $\langle c_k \rangle$  (of ion species  $k$ ) for pressure-driven flow,<sup>25</sup> as shown in Figure S1. Second, a flow through a charged channel can generate a streaming current, but the net current in the  $x$ -direction must be zero because the two ends are open. To offset the streaming current, a streaming potential will develop to push back cations and pull out anions from the charged channel, and this effect is magnified for multivalent cations. These two effects, the affinity for the charged channel where the velocity is low and stronger push-back by the streaming potential, make lead ions more difficult to remove from the charged channel to the outlet compared to sodium. Furthermore, the effects described above should be stronger for lower concentrations, as indicated by the larger magnitude of  $\beta_k^p$  at lower concentrations as shown in Figure S1, and a comparison between two simulation cases for different inlet concentrations is shown in Figure S2.

## CONCLUSION

We have shown that shock ED can selectively, effectively, and continuously remove lead simply by ion exchange (at zero current) or by electrokinetic transport at very low electrical energy costs. The experimental results are consistent with the predictions of a depth-averaged model well, which reveals the

mechanisms for selective multivalent ion removal. In future applications of the method, a reusable buffer solution could be used in place of acid for the electrode streams, and shock ED stacks could be built to further reduce the capital and operating costs.

## ASSOCIATED CONTENT

### Supporting Information

The Supporting Information is available free of charge at <https://pubs.acs.org/doi/10.1021/acsestwater.1c00234>.

Depth-averaged coefficient  $\beta_k^p$  for different ionic compositions (Figure S1), simulation results for different inlet concentrations (Figure S2), and simulation parameters (PDF)

## AUTHOR INFORMATION

### Corresponding Author

Martin Z. Bazant – Department of Chemical Engineering, Massachusetts Institute of Technology, Cambridge, Massachusetts 02139, United States; Department of Mathematics, Massachusetts Institute of Technology, Cambridge, Massachusetts 02139, United States; [orcid.org/0000-0002-8200-4501](https://orcid.org/0000-0002-8200-4501); Email: [bazant@mit.edu](mailto:bazant@mit.edu)

### Authors

Huanhuan Tian – Department of Chemical Engineering, Massachusetts Institute of Technology, Cambridge,

Massachusetts 02139, United States; [orcid.org/0000-0001-5515-9105](https://orcid.org/0000-0001-5515-9105)

**Mohammad A. Alkhadra** – Department of Chemical Engineering, Massachusetts Institute of Technology, Cambridge, Massachusetts 02139, United States; [orcid.org/0000-0003-3866-709X](https://orcid.org/0000-0003-3866-709X)

**Kameron M. Conforti** – Department of Chemical Engineering, Massachusetts Institute of Technology, Cambridge, Massachusetts 02139, United States

Complete contact information is available at:

<https://pubs.acs.org/10.1021/acsestwater.1c00234>

## Notes

The authors declare no competing financial interest.

## ACKNOWLEDGMENTS

H.T. acknowledges support from MathWorks Engineering Fellowship and a Graduate Student Fellowship awarded by the MIT Abdul Latif Jameel Water and Food Systems Lab and funded by Xylem, Inc. The authors thank the Center for Environmental Health Sciences (CEHS) at MIT for use of the ICP-MS instrument, and thank Saint Gobain Research North America for providing the SiC material.

## REFERENCES

- (1) Ryan, P. B.; Huet, N.; MacIntosh, D. L. Longitudinal investigation of exposure to arsenic, cadmium, and lead in drinking water. *Environ. Health Perspect.* **2000**, *108*, 731–735.
- (2) *Lead in Drinking Water*; World Health Organization, 2012.
- (3) Edwards, M.; Triantafyllidou, S.; Best, D. Elevated blood lead in young children due to lead-contaminated drinking water: Washington, DC, 2001–2004. *Environ. Sci. Technol.* **2009**, *43*, 1618–1623.
- (4) Brown, M. J.; Margolis, S. *Lead in drinking water and human blood lead levels in the United States*; Centers for Disease Control and Prevention, 2012.
- (5) Pieper, K. J.; Tang, M.; Edwards, M. A. Flint water crisis caused by interrupted corrosion control: investigating “ground zero” home. *Environ. Sci. Technol.* **2017**, *51*, 2007–2014.
- (6) Sanborn, L. H.; Carpenter, A. T. A progress report on efforts to address lead by public school districts. *J. - Am. Water Works Assoc.* **2018**, *110*, E18–E33.
- (7) Wang, T.; Kim, J.; Whelton, A. J. Management of plastic bottle and filter waste during the large-scale Flint Michigan lead contaminated drinking water incident. *Resources, Conservation and Recycling* **2019**, *140*, 115–124.
- (8) Vaishya, R. C.; Gupta, S. K. Coated sand filtration: an emerging technology for water treatment. *Aqua* **2003**, *52*, 299–306.
- (9) Esalah, J.; Husein, M. M. Removal of heavy metals from aqueous solutions by precipitation-filtration using novel organo-phosphorus ligands. *Sep. Sci. Technol.* **2008**, *43*, 3461–3475.
- (10) Yurekli, Y.; Yildirim, M.; Aydin, L.; Savran, M. Filtration and removal performances of membrane adsorbers. *J. Hazard. Mater.* **2017**, *332*, 33–41.
- (11) Ahmed, S.; Chughtai, S.; Keane, M. A. The removal of cadmium and lead from aqueous solution by ion exchange with Na–Y zeolite. *Sep. Purif. Technol.* **1998**, *13*, 57–64.
- (12) Chen, J. P.; Wang, L. Characterization of a Ca-alginate based ion-exchange resin and its applications in lead, copper, and zinc removal. *Sep. Sci. Technol.* **2001**, *36*, 3617–3637.
- (13) Petrus, R.; Warchol, J. K. Heavy metal removal by clinoptilolite. An equilibrium study in multi-component systems. *Water Res.* **2005**, *39*, 819–830.
- (14) Kurniawan, T. A.; Chan, G. Y.; Lo, W.-H.; Babel, S. Physico-chemical treatment techniques for wastewater laden with heavy metals. *Chem. Eng. J.* **2006**, *118*, 83–98.
- (15) Qiu, W.; Zheng, Y. Removal of lead, copper, nickel, cobalt, and zinc from water by a cancrinite-type zeolite synthesized from fly ash. *Chem. Eng. J.* **2009**, *145*, 483–488.
- (16) Kemmer, F. N.; McCallion, J. *The NALCO water handbook*; McGraw-Hill: New York, 1979.
- (17) Conforti, K. M.; Bazant, M. Z. Continuous ion-selective separations by shock electro dialysis. *AIChE J.* **2020**, *66*, No. e16751.
- (18) Schlumpberger, S.; Lu, N. B.; Suss, M. E.; Bazant, M. Z. Scalable and Continuous Water Deionization by Shock Electro dialysis. *Environ. Sci. Technol. Lett.* **2015**, *2*, 367–372.
- (19) Alkhadra, M. A.; Conforti, K. M.; Gao, T.; Tian, H.; Bazant, M. Z. Continuous Separation of Radionuclides from Contaminated Water by Shock Electro dialysis. *Environ. Sci. Technol.* **2020**, *54*, 527–536.
- (20) Alkhadra, M. A.; Gao, T.; Conforti, K. M.; Tian, H.; Bazant, M. Z. Small-scale desalination of seawater by shock electro dialysis. *Desalination* **2020**, *476*, 114219.
- (21) Dydek, E. V.; Zaltzman, B.; Rubinstein, I.; Deng, D.; Mani, A.; Bazant, M. Z. Overlimiting current in a microchannel. *Phys. Rev. Lett.* **2011**, *107*, 118301.
- (22) Mani, A.; Bazant, M. Z. Deionization shocks in microstructures. *Phys. Rev. E* **2011**, *84*, 061504.
- (23) Dydek, E. V.; Bazant, M. Z. Nonlinear dynamics of ion concentration polarization in porous media: The leaky membrane model. *AIChE J.* **2013**, *59*, 3539–3555.
- (24) Schlumpberger, S.; Smith, R. B.; Tian, H.; Mani, A.; Bazant, M. Z. Deionization shocks in crossflow. *AIChE J.* **2021**, *67*, e17274.
- (25) Tian, H.; Alkhadra, M. A.; Bazant, M. Z. Theory of shock electro dialysis I: Water dissociation and electrosmotic vortices. *J. Colloid Interface Sci.* **2021**, *589*, 605–615.
- (26) Tian, H.; Alkhadra, M. A.; Bazant, M. Z. Theory of shock electro dialysis II: Mechanisms of selective ion removal. *J. Colloid Interface Sci.* **2021**, *589*, 616–621.
- (27) Roy, S. Lead Results from Tap Water Sampling in Flint, MI During the Flint Water Crisis. Flint Water Study Updates, December 2015, 1.
- (28) City of Flint 2017 Annual Water Quality Report. City of Flint, 2012.
- (29) Tian, H.; Wang, M. Electrokinetic mechanism of wettability alteration at oil-water-rock interface. *Surf. Sci. Rep.* **2017**, *72*, 369–391.